



## Transitions in the Parameter Space of a Periodically Forced Dissipative System

K. ULLMANN and I. L. CALDAS

Instituto de Física da Universidade de São Paulo, C. P. 66318, 05389-970 São Paulo, Brazil

(Accepted 28 February 1996)

**Abstract**—Transitions between periodic, quasiperiodic and chaotic regions in the parameter space of a dissipative integrable system, periodically perturbed by delta-peaks, are numerically investigated in the limit of fast relaxation. Lyapunov exponents, winding numbers, power spectra and isoperiodic diagrams are computed to analyse the different kinds of transitions and their characteristics as the control parameters, the perturbation amplitude and period, are varied. Copyright © 1996 Elsevier Science Ltd.

### INTRODUCTION

Dynamical systems and their applications have been extensively studied in the past few years [1, 2]. In particular, nonlinear systems leading to chaotic behaviour have been intensively examined [3–5], with particular emphasis on systems such as relaxation oscillators subject to external perturbations, periodic or not [6, 7]. More recently, various methods for controlling chaos have been developed, including many which use small external perturbations [8].

Within dynamical systems in general, mappings (that is, systems whose temporal evolution can be computed by discrete iterations) were subject to special interest, both multi-dimensional (Henon map, Chirikov map, baker map, . . .) and one-dimensional maps (quadratic map, circle maps, . . .) [2, 9]. These maps are quite important because of their simple properties, which permit a clear identification of the different phenomena which occur in dynamical systems. Some of them still describe with some accuracy real systems of interest such as population growth [10], neural dynamics [11], hiccups [12], tremors [13], etc.

Many important concepts were introduced by such mappings [14], and they present phenomena such as the known routes leading to chaos, fractal attractor basins and phase-locking, for example. Even some universal behaviours, such as the Feigenbaum route and its constants in the quadratic maps [10], were discovered.

For purposes of qualitative behaviour studies, as in many cases the mappings are simpler to analyse than continuously evolving systems, sometimes the latter are reduced to maps in limit cases or with some approximations, using for example Dirac's delta function for the description of impulsive perturbations. Hence, there are some quite sophisticated mappings nowadays describing complex real systems with great accuracy [15, 16].

In this work we consider a class of two-dimensional autonomous integrable systems, perturbed by delta-peaks in a fixed direction (chosen to be the  $x$ -axis), given by [17]:

$$\frac{dx}{dt} = sx(1 - x^2 - y^2) - y + 2a \sum_n \delta(t - 2\pi nb) \quad (1a)$$

$$\frac{dy}{dt} = sy(1 - x^2 - y^2) + x \tag{1b}$$

where  $s$  is a relaxation parameter,  $2a$  is the intensity and  $2\pi b$  is the period of the perturbation delta-peaks along the  $x$ -direction. In the absence of perturbation ( $a = 0$ ) the system above is integrable and presents a stable limit-cycle with a unitary radius and an unstable fixed point at  $r = 0$ . Systems of this kind (stable limit-cycle containing unstable fixed point), known in the literature as soft oscillators, are widely studied [7].

For fast relaxation ( $s \gg 1$ ) the system returns to the limit-cycle almost immediately after each kick and so the system, in this fast relaxation limit, can be described by the one-dimensional map [17]:

$$\tan \theta_{n+1} = \frac{\sin(\theta_n + 2\pi b)}{2a + \cos(\theta_n + 2\pi b)} \tag{2}$$

given in polar coordinates  $r$  and  $\theta$  ( $x = r \cos \theta$ ,  $y = r \sin \theta$ ), where  $\theta_n$  is defined as the polar angle immediately after the  $n$ th kick at time  $t = 2\pi nb$ . In this case we always have  $r_n = 1$ . In this paper we study this one-dimensional map in the control parameter space  $a \times b$ , trying to enlighten the transitions between the different kinds of possible dynamical behaviour (periodic, quasiperiodic and chaotic).

### THE PARAMETER PLANE

The region of the parameter space which is of physical interest is delimited by  $a > 0$  and  $0 < b < 1$ . Numerical investigation has shown that the dynamical behaviour of the system here considered presents a symmetry axis at  $b = \frac{1}{2}$ , so we will study only the region of the parameter plane with  $0 < b < \frac{1}{2}$ . Within these limits there are three distinct regions of the parameter space which present distinct dynamical properties.

(i) The region of weak perturbation intensity ( $0 < a < \frac{1}{2}$ ) where the uni-dimensional map (2) is invertible and therefore no chaotic behaviour can exist, so the trajectories can be classified as periodical or quasi-periodical. Figure 1(a) shows an isoperiodic diagram

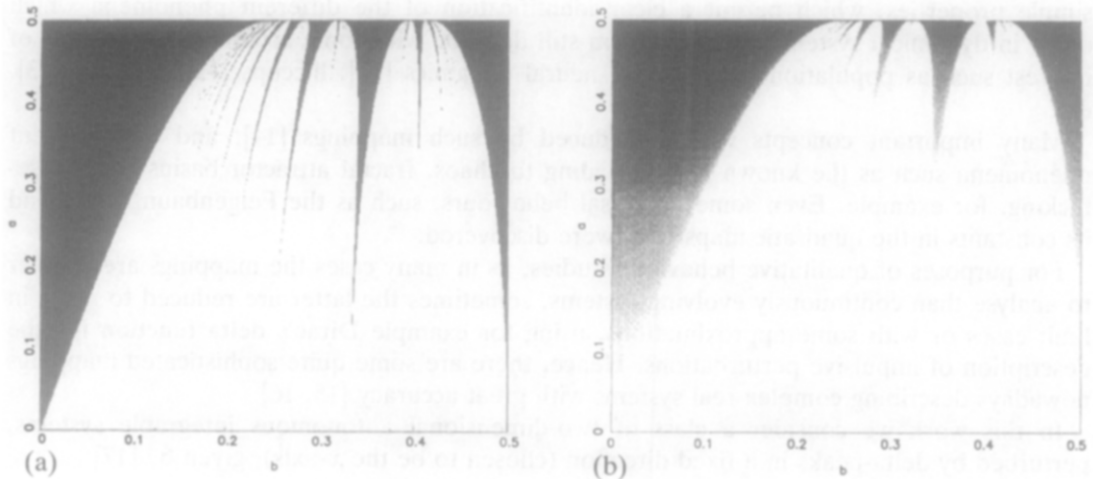


Fig. 1. (a) Isoperiodic diagram with dark regions corresponding to the main periods; and (b) Lyapunov exponents with white regions corresponding to  $\lambda = 0$  and dark to  $\lambda < 0$ .

[18, 19] of this region of the parameter plane. It consists of computing trajectories, for fixed parameter values of  $(a, b)$ , and plotting differently grey-shaded points on the plane, corresponding to different periodicities of the system, leaving in blank the points corresponding to quasiperiodical trajectories. Thus, we obtain a well-known pattern usually called ‘Arnold tongues’ or ‘Arnold sausages’ in the literature [20, 21]. This is characteristic of systems presenting mode-locking, as the circle map [22], which is a limit of our map for very low perturbation intensities ( $a \ll 1$ ). We also plotted the Lyapunov exponents (Fig. 1(b)), which for one-dimensional maps are defined as:

$$\lambda \equiv \lim_{N \rightarrow \infty} \frac{1}{N} \sum_{j=0}^N \ln \left\| \frac{\partial \theta_{j+1}}{\partial \theta_j} \right\| \quad (3)$$

and we have that  $\lambda < 0$  corresponds to periodical,  $\lambda = 0$  to quasiperiodical, and  $\lambda > 0$  to chaotic trajectories. Here we see again the ‘Arnold tongues’ in accordance with the isoperiodic diagram and we can also observe that the Lyapunov exponents are the more negative as the point in the parameter plane is more distant to the next quasiperiodic point.

(ii) The region of stronger perturbation ( $\frac{1}{2} < a < 1$ ), where the map is no longer invertible, contains regions of chaotic behaviour, as we can see in the isoperiodic diagram (Fig. 2(a)). For this region, as there are no trajectories with quasiperiodical behaviour, we assigned blank regions in the isoperiodic diagram to chaotic trajectories. Plotting also the Lyapunov exponents for this region (Fig. 2(b)), we can see the complex behaviour of the boundaries of the chaotic region. There are also light bands in the periodic regions of the parameter plane, characterized by  $\lambda = 0$  corresponding to the points where the period-doubling occurs. They form sequences which are among the well-known routes leading to chaos in literature [2, 3]. Magnifying a region of the isoperiodic diagram (Fig. 3(a)) and of the Lyapunov exponents plot (Fig. 3(b)), where the periodic bands with distinct periods cross each other, we can see a fractal superposition of the different periodic attractors. This is the only region of the parameter plane where the final behaviour of the system is sensible to the initial condition, as we will show in more detail later.

(iii) The region of very strong perturbation ( $a > 1$ ) where there is only periodic

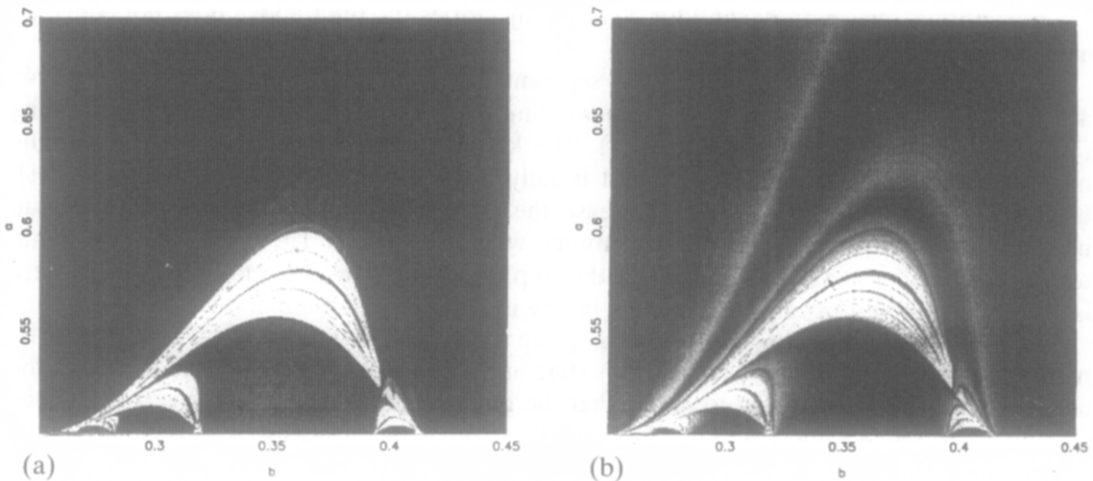


Fig. 2. (a) Isoperiodic diagram around the chaotic region with white points at aperiodic orbits; and (b) Lyapunov exponents with light points for  $\lambda > 0$  and dark points for  $\lambda < 0$ .

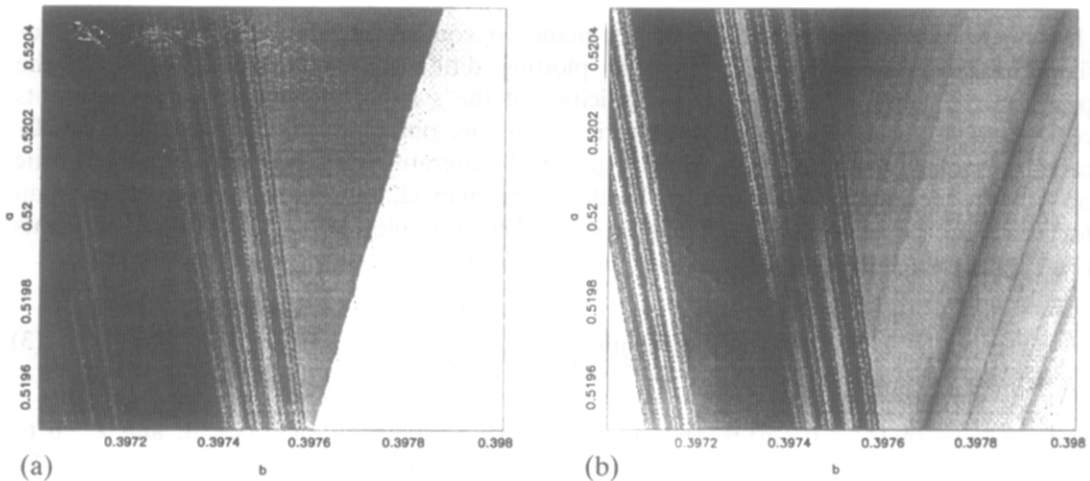


Fig. 3. Magnification of details from Fig. 2.

that the original system's characteristics can no longer be observed. Also the physical reality of a system returning quite immediately to its limit-cycle after so strong a perturbation is very questionable.

### TRANSITIONS BETWEEN PERIODIC AND QUASIPERIODIC REGIMES

For a better understanding of the transitions between the periodical and quasiperiodical regimes in the parameter space we are going to present a numerical example. For this we define the winding number, widely used in dynamical analysis [3], given by:

$$W \equiv \lim_{N \rightarrow \infty} \frac{1}{N} \sum_{j=0}^N (\theta_{j+1} - \theta_j). \quad (4)$$

If the trajectories are periodic then  $W$  is a rational number and can hence be written as  $W = p/q$  ( $q \neq 0$ ), where  $q$  is the period of the trajectory. For irrational winding numbers the trajectory is quasiperiodic and for chaotic trajectories the limit above does not converge and so there exists no winding number.

As a numerical example a straight line segment in the parameter plane given by  $a = 0.45$  and  $0.25 < b < 0.50$  was chosen, and the winding numbers and Lyapunov exponents along this line segment were computed (Fig. 4). The kind of graph we obtained for the winding numbers is well known in literature and usually denominated the 'Devil's' staircase [21], because it is always growing as we increase the period of the perturbation and forms an infinite number of steps, one for each rational winding number. The larger the denominator of this winding number the narrower the step and so it forms a fractal structure as there is an infinite amount of rational numbers in any interval of real numbers.

The plot of the Lyapunov exponents is given by a straight line at  $\lambda = 0$  interrupted by negative gaps for each step of the 'Devil's staircase'. The broader the step the deeper is the associated gap. It is important to notice that the gradient of the Lyapunov is very large (the line in the graph is almost vertical) only in the vicinity of quasiperiodical regimes. For a better understanding of the transition between the first two great gaps (or steps), corresponding, respectively, to periods 4 and 5, we computed several power spectra [23] along our line segment (Fig. 5), using the FFT algorithm [24] with  $N = 2^{14}$  trajectory points

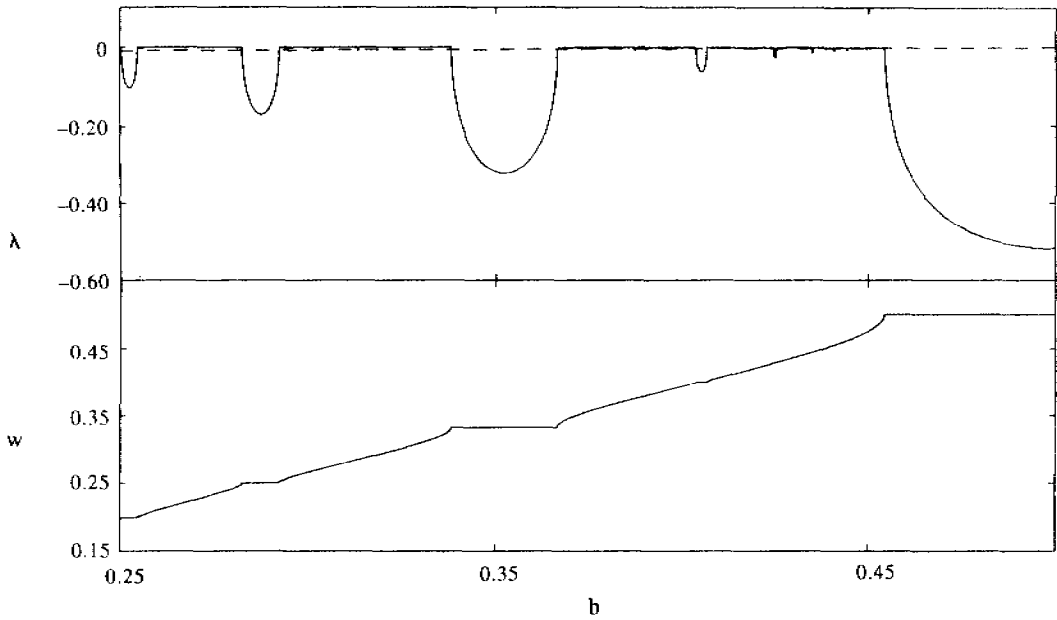


Fig. 4. Lyapunov exponents and winding numbers fixing  $a = 0.45$  and varying the control parameter  $b$ .

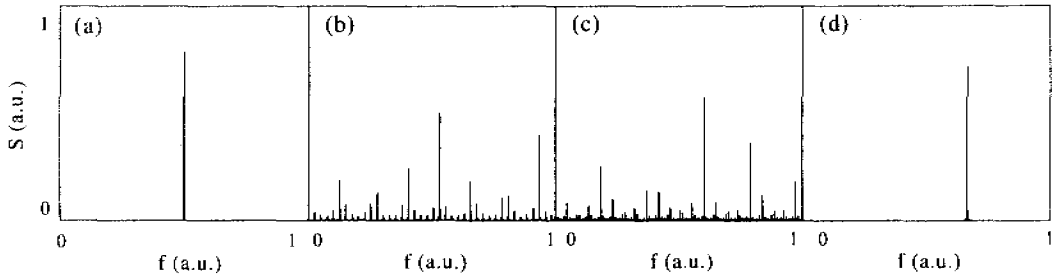


Fig. 5. Power spectra fixing  $a = 0.45$  and (a)  $b = 0.286$ ; (b)  $b = 0.300$ ; (c)  $b = 0.325$ ; (d)  $b = 0.350$ .

for each spectrum. The spectra of the periodic regimes both have only a discrete number of sharp peaks, while the power spectra of the quasiperiodical trajectories have an infinite number of sharp peaks. Observing the largest of these peaks, as we vary the control parameter  $b$ , we observe that they are shifting continuously between the positions of the final periods on the frequency axis. So we can see that this kind of transition is characterized by a continuous process of frequency shifting and splitting around the main frequencies as we vary the parameters.

### TRANSITIONS BETWEEN PERIODIC AND CHAOTIC REGIMES

For studying the transition between periodic and chaotic regimes, which occurs in the parameter plane for stronger perturbations, we have chosen as a numerical example the straight line segment defined by  $a = 0.57$  and  $0.25 < b < 0.50$ . Figure 6(a) shows the Lyapunov exponents along this line segment and the bifurcation diagram (Fig. 6(b)), which consists of plotting for each fixed  $b$  all angles  $\theta_n^*$  passed by the system after the transient. We can see that as we increase  $b$  the system passes from periodic behaviour of period 1 to

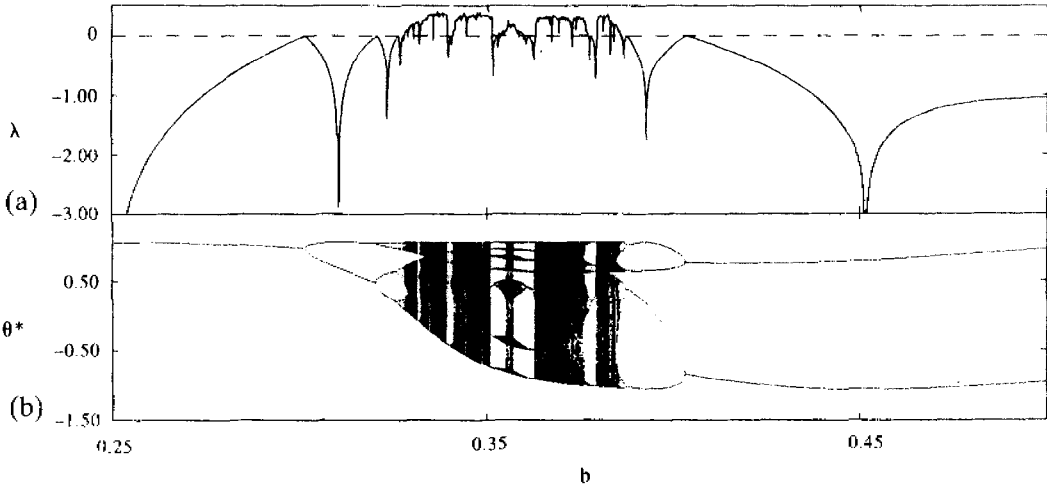


Fig. 6. Lyapunov exponents and bifurcation diagram fixing  $a = 0.57$  and varying the control parameter  $b$ .

chaos by successive period-doubling bifurcations. In the chaotic regime there can be observed several windows of periodic behaviour with several different periods and then the system passes to periodic behaviour with period 2 via a reverse bifurcation process. The period-doubling route to chaos here observed is one of the standard routes and has been frequently observed in a lot of different systems [2, 3, 5].

Computing several power spectra along this transition for fixed values of  $b$  (Fig. 7) we observe that as the bifurcations occur new sharp spectral peaks begin to grow, corresponding to the new periods generated by bifurcations. As we enter the chaotic region these peaks are still dominant until a region where the crises have merged all chaotic bands to only one. In this region only a continuous spectrum with no dominant sharp peaks remains.

It is interesting to notice that in this kind of transition the main peaks do not move along the frequency axis as we vary the control parameters but have fixed positions. So we have no frequency shifting, chaos being generated by the superposition of an infinite number of periodic peaks which grow and decrease as the transition occurs. This transition is associated to a boundary crisis [23].

### TRANSITIONS BETWEEN PERIODIC REGIMES OF NON-COMENSURABLE PERIODS

The third and last kind of transition we analysed can only be observed in very small regions of the parameter plane and is given by the direct transition between non-comensurable periods. Differently from the transition between comensurable periods, which occurs

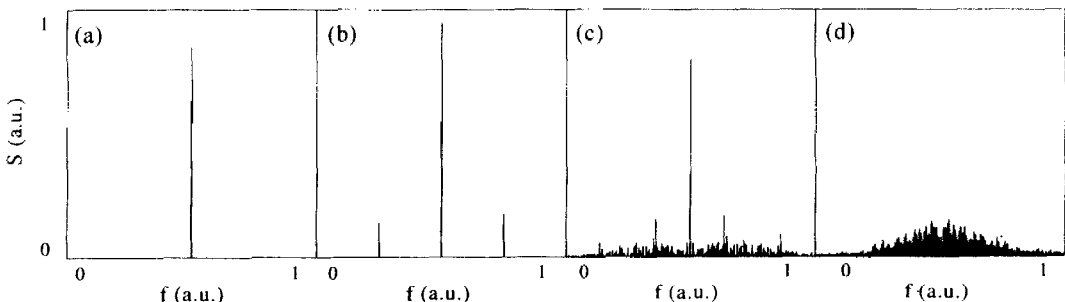


Fig. 7. Power spectra fixing  $a = 0.57$  and (a)  $b = 0.325$ ; (b)  $b = 0.327$ ; (c)  $b = 0.329$ ; (d)  $b = 0.331$ .

during the period-doubling process which leads to chaos, this kind of transition occurs by the encounter of periodic tongues with non-commensurable periods at the edges of the chaotic regions.

For a numerical study of this kind of transition we have chosen the straight line segment in the parameter plane given by  $a = 0.52$  and  $0.397 < b < 0.398$ , where the superposition of a period-3 tongue with a period-doubling transition of the kind (4-8-16-...) occurs. Plotting the Lyapunov exponents along this line segment (Fig. 8(a)) we can observe that the plot consists of the fractal intercalation of two distinct curves: one of the period-3 attractor and the other of the period-doubling leading to chaos. The transition between the curves is abrupt. Plotting the winding numbers for this transition (Fig. 8(b)) we observe the same abrupt fractal behaviour as in the case of Lyapunov exponents, but the plot oscillates now between two horizontal lines, one at  $W = \frac{1}{3}$  (period 3) and the other at  $W = \frac{1}{4}$  (periods 4-8-16-...), until with increasing  $b$  we enter chaos and  $W$  no longer converges. Plotting, finally, the bifurcation diagram for this case (Fig. 8(c)) we observe once more the fractal superposition of the two kinds of behaviour as we vary the perturbation parameter  $b$ . We have also plotted the winding numbers for this kind of transition fixing  $b = 0.3975$  and varying the initial angular position (Fig. 9). Here we observe that the fractal interlacing of the attractor basins occurs also in phase space, not only in the parameter space.

So we observe that this kind of transition is characterized by the fractal superposition of two basins of attraction and the transition from one basin to another is an abrupt process.

### CONCLUSIONS

The three kinds of transitions in the parameter plane discussed above are of very different nature. The transition between periodic and quasiperiodic behaviour is generated by a continuous shifting of frequencies, the transition between periodic and chaotic trajectories is given by growing and decreasing of fixed frequency peaks and the transition

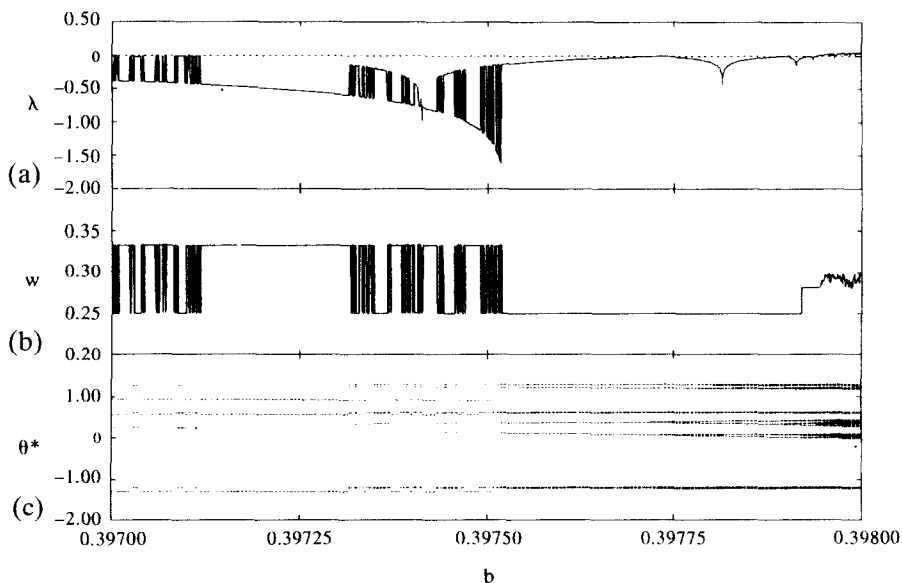


Fig. 8. Lyapunov exponents, winding numbers, and bifurcation diagram fixing  $a = 0.520$  and varying the control parameter  $b$ .

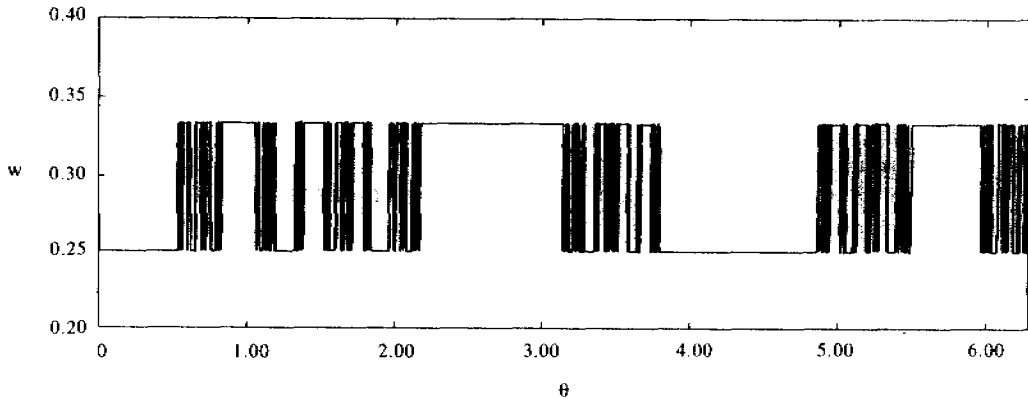


Fig. 9. Winding numbers fixing  $a = 0.5200$ ,  $b = 0.3975$ , and varying the initial angle  $\theta$ .

between two non-commensurable periods is generated by the fractal superposition of both attractor basins. This fractality can be observed both in the parameter space and in the phase space.

As our system is a prototype for soft oscillators, we can apply these results as a diagnosis of mode-locking behaviour and period-doubling bifurcations leading to chaos in experimental systems with strong relaxation just measuring frequency power spectra for some fixed values of the external perturbation parameters.

*Acknowledgements*—Work partially supported by CNPq and FAPESP (Brazilian Government Agencies). Useful discussions with Prof. Dr C. Grebogi (University of Maryland at College Park) and Prof. Dr R. L. Viana (Federal University of Paraná, Curitiba) are acknowledged.

## REFERENCES

1. C. Grebogi, E. Ott and J. A. Yorke, Chaos, strange attractors and fractal basin boundaries in nonlinear dynamics, *Science* **238**, 632–638 (1987).
2. P. Cvitanovic (Ed.), *Universality in Chaos*. Adam Hilger, Bristol (1989).
3. E. Ott, *Dynamical Systems*. Cambridge University Press, Cambridge (1993).
4. J. P. Keener and L. Glass, Global bifurcations of a periodically forced nonlinear oscillator, *J. Math. Biology* **21**, 175–190 (1984).
5. T. Kapitaniak and M. S. El Naschie, A note on randomness and strange behaviour, *Phys. Lett. A* **154**, 249–253 (1991).
6. T. Kapitaniak (Ed.), *Chaotic Oscillators*. World Scientific, Singapore (1991).
7. G. A. Cecchi, D. L. Gonzalez, M. O. Magnasco, G. B. Midlin, O. Piro and A. J. Santillan, Periodically kicked hard oscillators, *Chaos* **3**, 51–62 (1993).
8. T. Shinbrot, C. Grebogi, E. Ott and A. Yorke, Using small perturbations to control chaos, *Nature* **363**, 411–417 (1993).
9. H. G. Schuster, *Deterministic Chaos*. Physik Verlag, Berlin (1984).
10. M. Markus, Chaos in maps with continuous and discontinuous maxima, *Computers in Physics* **5**, 481–493 (1990).
11. M. Zeller, M. Bauer and W. Martienssen, Neural dynamics modelled by one-dimensional circle maps, *Chaos, Solitons & Fractals* **5**, 885–893 (1995).
12. W. A. Whitelaw, J.-Ph. Derenne and J. Cabane, Hiccups as a dynamical disease, *Chaos* **5**, 14–17 (1995).
13. A. Bosse, Ch. Jentgens, S. Spieker and J. Dichgans, Variations on tremor parameters, *Chaos* **5**, 52–56 (1995).
14. S. Bahar, Chaotic orbits and bifurcation from a fixed point generated by an iterated function system, *Chaos, Solitons & Fractals* **5**, 1001–1006 (1995).
15. T. J. Martin and J. B. Taylor, Ergodic behaviour in a magnetic limiter, *Plasma Phys. Contr. Fus.* **26**, 321 (1984).
16. I. L. Caldas, J. M. Pereira, K. Ullmann and R. L. Viana, Magnetic field line mappings for a Tokamak with ergodic limiters, *Chaos, Solitons & Fractals* **7**, 991–1010 (1996).
17. E. J. Ding, Analytic treatment of periodic orbit systematics for a nonlinear driven oscillator, *Phys. Rev. A* **34**, 3547–3550 (1986).

18. J. A. C. Gallas, Structure of the parameter space of the Hénon map, *Phys. Rev. Lett.* **70**, 2714–2717 (1993).
19. J. A. C. Gallas, C. Grebogi and J. A. Yorke, Vertices in parameter space: Double crises which destroy chaotic attractors, *Phys. Rev. Lett.* **71**, 1359–1362 (1993).
20. W. Yang and B. Hao, How the Arnold tongues become sausages in a piecewise linear circle map, *Com. Theor. Phys.* **8**, 1–15 (1987).
21. P. Bak, The devil's staircase, *Physics Today* **39**, 38–45 (1986).
22. J. M. Greene, A method for determining a stochastic transition, *J. Math. Phys.* **20**, 1183–1201 (1979).
23. F. Romeiras, C. Grebogi and E. Ott, Critical exponents for power-spectra scaling at merging of chaotic bands, *Phys. Rev. A* **38**, 463–468 (1988).
24. R. W. Hamming, *Numerical Methods for Scientists and Engineers*. Dover Publications Inc., New York (1989).